

Supporting Information

Synthesis and Characterisation of Tetranuclear Ruthenium Polyhydrido Clusters with Pseudo-Tetrahedral Geometry

Hajime Kameo,^a Yutaka Ito,^a Ryuichi Shimogawa,^a Asuka Koizumi,^a Hiroki Chikamori,^a
Junko Fujimoto,^a Hiroharu Suzuki,^{a,*} and Toshiro Takao^{a,b,*}

^a *Department of Chemical Science and Engineering, School of Materials and Chemical Technology, Tokyo Institute of Technology, 2-12-1 O-okayama, Meguro-ku, Tokyo 152-8552, Japan Address here.*

^b *JST, ACT-C, 4-1-8 Honcho, Kawaguchi, Saitama 3332-0012, Japan.*

Contents

1. Crystal data and results of XRD studies for **5**, **7**, **8**, **8'**, and **10'**
2. NMR spectra of **5-BF₄**, **5-BPh₄**, **5'-BF₄**, **7-BF₄**, **7-BPh₄**, **7'-BF₄**, **8**, **8'**, and **10'**
3. Results of DFT calculations for **5''-A**, **5''-B**, **7''**, **8''**, and **10''**

1. Crystal data and results of XRD studies for **5**, **7**, **8**, **8'**, and **10'**

Table S-1. Crystallographic Data for **5**, **7**, **8**, **8'**, and **10'**

	5	7	8	8'	10'
Formula	C ₉₀ H ₁₁₄ B ₂ N ₂ O ₄ Ru ₄	C ₆₄ H ₈₇ B Ru ₄	C ₄₀ H ₆₆ Ru ₄	C ₄₄ H ₇₄ Ru ₄	C ₄₄ H ₇₂ Ru ₄
Formula weight	1713.73	1271.43	951.20	1007.31	1005.29
Crystal description	platelet	block	block	needle	block
Crystal color	black	black	black	black	black
Crystal size (mm)	0.429×0.397×0.086	0.372×0.119×0.086	0.145×0.137×0.118	0.211×0.124×0.100	0.341×0.133×0.131
Crystallizing solution	CH ₃ NO ₂ /CH ₃ OH (25 °C)	Acetone/Et ₂ O (25 °C.)	THF (70 °C)	Hexane (−30 °C)	Hexane (−30 °C)
Crystal system	monoclinic	monoclinic	triclinic	orthorhombic	orthorhombic
Space group	<i>P2₁/c</i> (#14)	<i>P2₁/c</i> (#14)	<i>P</i> -1 (#2)	<i>Pnma</i> (#62)	<i>Pnma</i> (#62)
<i>a</i> (Å)	23.6293(7)	16.8721(5)	10.8082(4)	15.3508(6)	15.2441(3)
<i>b</i> (Å)	19.3197(6)	20.1549(6)	10.8464(3)	17.1336(6)	17.0861(5)
<i>c</i> (Å)	17.7321(5)	17.1805(5)	18.0784(7)	16.1327(6)	16.0747(3)
α (°)			83.5770(10)		
β (°)	95.691(7)	93.491(7)	84.2980(10)		
γ (°)			66.7760(10)		
<i>V</i> (Å ³)	8055.0(4)	5831.5(3)	1931.83(12)	4243.1(3)	4186.85(17)
<i>Z</i> value	4	4	2	4	4
<i>D</i> _{calcd} (g/cm ³)	1.413	1.053	1.635	1.577	1.595
Measurement temp. (°C)	−120	−120	−150	−120	−120
μ (MoK α) (mm ^{−1})	0.787	1.513	1.559	1.425	1.444
$2\theta_{\max}$ (deg)	55.0	55.0	55	55	55
No. of reflections collected	77914	56383	19142	66543	44573
No. of unique reflections	18394 (<i>R</i> _{int} = 0.0792)	13323 (<i>R</i> _{int} = 0.0573)	8661 (<i>R</i> _{int} = 0.0349)	5007 (<i>R</i> _{int} = 0.0963)	4934 (<i>R</i> _{int} = 0.0888)
No. Reflections observed (>2 σ)	15395	11190	6977	4488	4777
Abs. correction type	Empirical	Empirical	Empirical	Numerical	Numerical
Abs. transmission	0.6736(min.) 1.000(max.)	0.7176 (min.) 1.0000 (max.)	0.7423 (min.) 1.0000 (max.)	0.8179 (min.) 0.9153 (max.)	0.7186 (min.) 0.8436 (max.)
<i>R</i> ₁ [<i>I</i> > 2 σ (<i>I</i>)]	0.0387	0.0368	0.0356	0.0313	0.0263
<i>wR</i> ₂ [<i>I</i> > 2 σ (<i>I</i>)]	0.0917	0.0776	0.0942	0.0742	0.0689
<i>R</i> ₁ (all data)	0.0500	0.0489	0.0471	0.0359	0.0272
<i>wR</i> ₂ (all data)	0.0968	0.0816	0.1024	0.0764	0.0696
Data / restraints / parameters	18394 / 0 / 974	13323 / 0 / 766	8661 / 0 / 381	5007 / 0 / 260	4934 / 0 / 249
Goodness of fit on <i>F</i> ²	1.020	1.068	1.092	1.047	1.015
Largest diff. peak and hole (e [−] Å ^{−3})	1.142 and −1.115	1.364 and −0.929	1.801 and −1.252	0.759 and −0.789	0.717 and −0.604

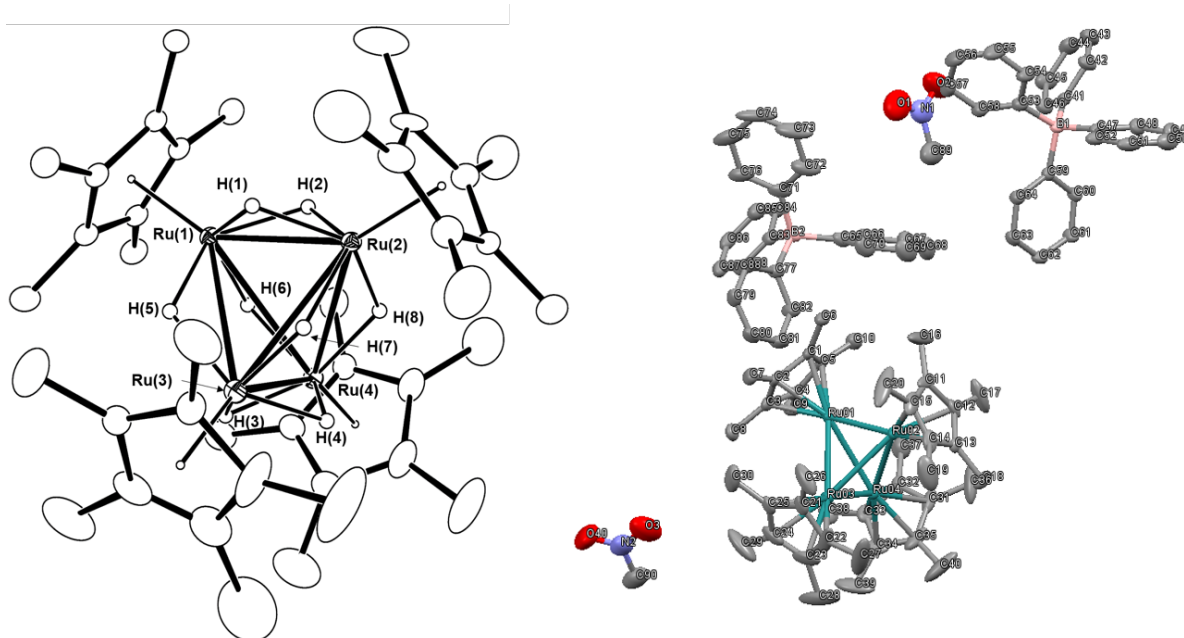


Figure S-1. ORTEP diagram of the cationic part of $[(\text{Cp}^*\text{Ru})_4\text{H}_8]^{2+}(\text{BPh}_4^-)_2$ (**5-BPh₄**), with thermal ellipsoids drawn at 30% probability (left), and the structure of a tetraphenylborate salt of **5** (right). Hydrogen atoms on the Cp* groups were omitted for clarity.

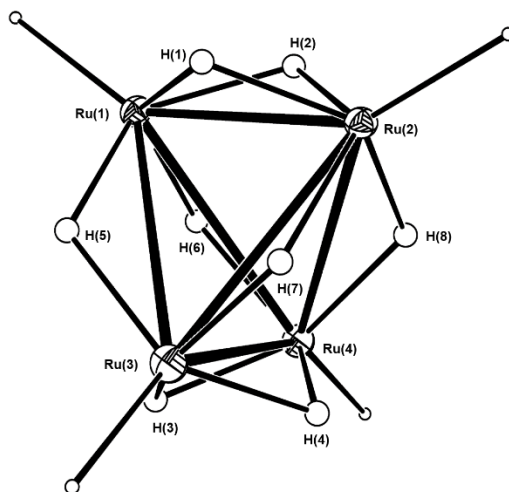


Figure S-2. Expanded view of the Ru_4 core of **5-BPh₄**

Table S-2. Selected bond lengths (Å) and angles (deg) of **5-BPh₄**

Ru(1)–Ru(2)	2.6684(3)	Ru(1)–Ru(3)	3.0382(3)	Ru(1)–Ru(4)	3.0323(3)
Ru(2)–Ru(3)	3.0428(3)	Ru(2)–Ru(4)	3.0535(3)	Ru(3)–Ru(4)	2.6751(3)
Ru(2)–Ru(1)–Ru(3)	64.061(8)	Ru(2)–Ru(1)–Ru(4)	64.405(8)	Ru(3)–Ru(1)–Ru(4)	52.293(7)
Ru(1)–Ru(2)–Ru(3)	63.883(8)	Ru(1)–Ru(2)–Ru(4)	63.585(8)	Ru(3)–Ru(2)–Ru(4)	52.054(7)
Ru(1)–Ru(3)–Ru(2)	52.056(7)	Ru(1)–Ru(3)–Ru(4)	63.741(9)	Ru(2)–Ru(3)–Ru(4)	64.180(10)
Ru(1)–Ru(4)–Ru(2)	52.010(7)	Ru(1)–Ru(4)–Ru(3)	63.967(8)	Ru(2)–Ru(4)–Ru(3)	63.766(10)

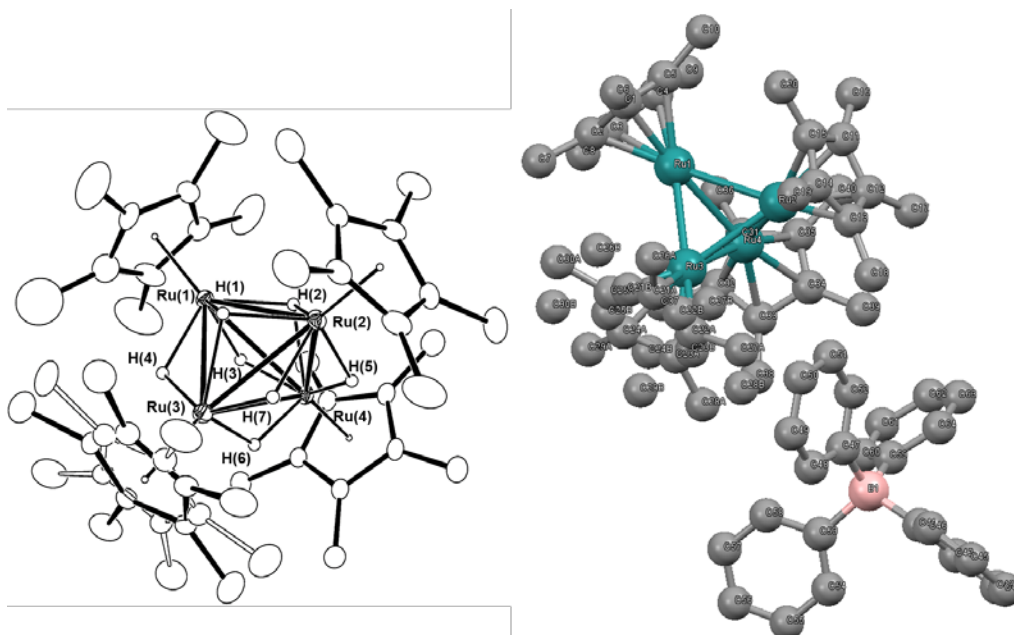


Figure S-3. ORTEP diagram of the cationic part of $[(\text{Cp}^*\text{Ru})_4\text{H}_7]^+(\text{BPh}_4^-)$ (**7-BPh₄**), with thermal ellipsoids drawn at 30% probability (left), and the structure of a tetraphenylborate salt of **5** (right). Hydrogen atoms on the Cp* groups were omitted for clarity.

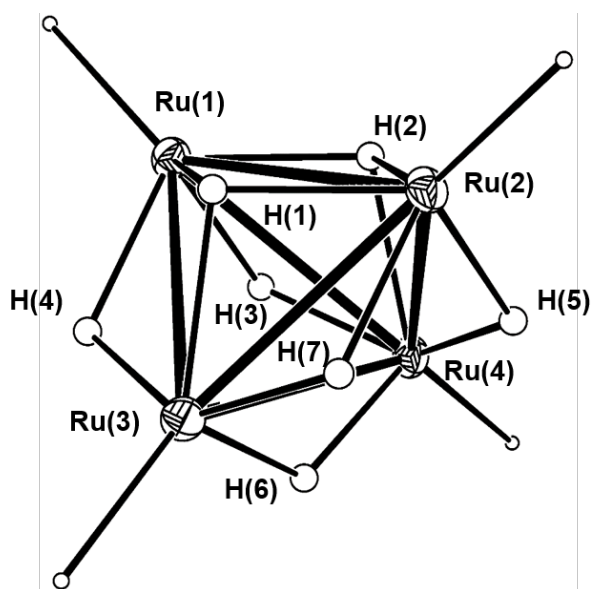


Figure S-4. Expanded view of the Ru_4 core of **7-BPh₄**

Table S-3. Selected bond lengths (Å) and angles (deg) of **7-BPh₄**

Ru(1)–Ru(2)	3.0006(4)	Ru(1)–Ru(3)	2.8474(4)	Ru(1)–Ru(4)	2.8207(3)
Ru(2)–Ru(3)	2.8034(3)	Ru(2)–Ru(4)	2.8429(3)	Ru(3)–Ru(4)	2.9870(4)
Ru(2)–Ru(1)–Ru(3)	57.216(8)	Ru(2)–Ru(1)–Ru(4)	58.367(9)	Ru(3)–Ru(1)–Ru(4)	63.604(11)
Ru(1)–Ru(2)–Ru(3)	58.641(8)	Ru(1)–Ru(2)–Ru(4)	57.649(8)	Ru(3)–Ru(2)–Ru(4)	63.876(10)
Ru(1)–Ru(3)–Ru(2)	64.143(9)	Ru(1)–Ru(3)–Ru(4)	57.77(1)	Ru(2)–Ru(3)–Ru(4)	58.71(1)
Ru(1)–Ru(4)–Ru(2)	63.99(1)	Ru(1)–Ru(4)–Ru(3)	58.633(8)	Ru(2)–Ru(4)–Ru(3)	57.418(8)

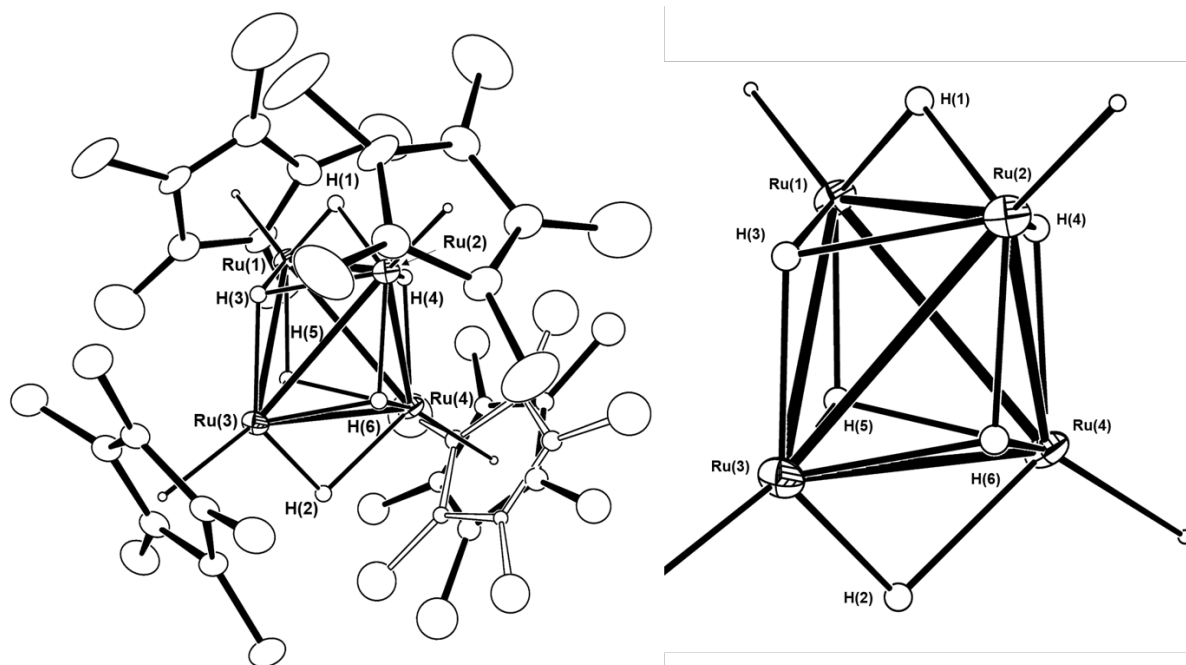


Figure S-5. ORTEP diagram of $[(\text{Cp}^*\text{Ru})_4\text{H}_6]$ (**8**), with thermal ellipsoids drawn at 30% probability (left), and the expanded view of the Ru_4 core of **8** (right). Hydrogen atoms on the Cp^* groups were omitted for clarity.

Table S-4. Selected bond lengths (\AA) and angles (deg) of **8**

Ru(1)–Ru(2)	2.7482(4)	Ru(1)–Ru(3)	2.9568(4)	Ru(1)–Ru(4)	2.9743(4)
Ru(2)–Ru(3)	2.9861(4)	Ru(2)–Ru(4)	2.9787(4)	Ru(3)–Ru(4)	2.7400(5)
Ru(2)–Ru(1)–Ru(3)	62.999(11)	Ru(2)–Ru(1)–Ru(4)	62.587(11)	Ru(3)–Ru(1)–Ru(4)	55.028(10)
Ru(1)–Ru(2)–Ru(3)	61.915(11)	Ru(1)–Ru(2)–Ru(4)	62.425(11)	Ru(3)–Ru(2)–Ru(4)	54.692(10)
Ru(1)–Ru(3)–Ru(2)	55.085(10)	Ru(1)–Ru(3)–Ru(4)	62.810(11)	Ru(2)–Ru(3)–Ru(4)	62.515(11)
Ru(1)–Ru(4)–Ru(2)	54.99(1)	Ru(1)–Ru(4)–Ru(3)	62.162(11)	Ru(2)–Ru(4)–Ru(3)	62.79(1)

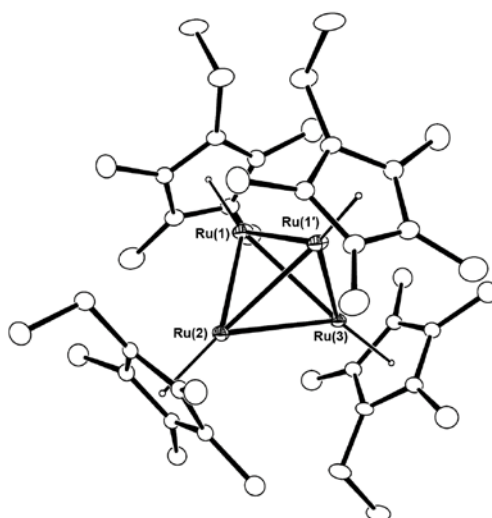
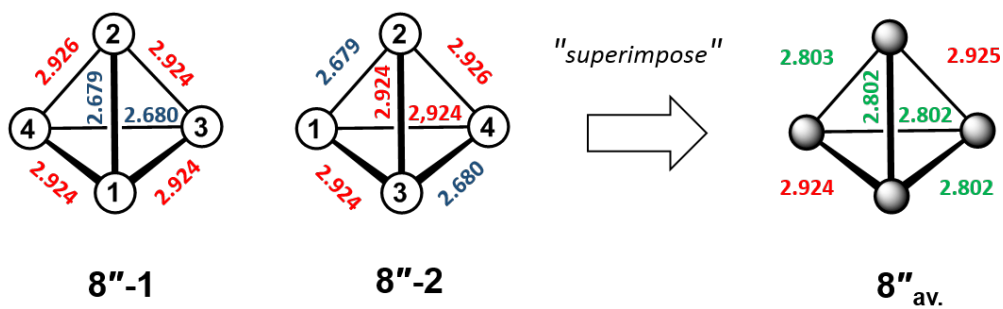


Figure S-6. ORTEP diagram of $[(\text{Cp}^{\text{Et}}\text{Ru})_4\text{H}_6]$ (**8'**), with thermal ellipsoids drawn at 30% probability. Hydrogen atoms on the Cp^{Et} groups were omitted for clarity.

Table S-5. Selected bond lengths (\AA) and angles (deg) of **8'**

Ru(1)–Ru(1')	2.9841(4)	Ru(1)–Ru(2)	2.8670(3)	Ru(1)–Ru(3)	2.8693(3)
Ru(2)–Ru(3)	2.9695(4)				
Ru(1')–Ru(1)–Ru(2)	58.638(6)	Ru(1')–Ru(1)–Ru(3)	58.666(5)	Ru(2)–Ru(1)–Ru(3)	62.351(9)
Ru(1)–Ru(2)–Ru(1')	62.722(11)	Ru(1)–Ru(2)–Ru(3)	58.863(8)	Ru(1)–Ru(3)–Ru(1')	62.665(11)
Ru(1)–Ru(3)–Ru(2)	58.785(8)				



Scheme S-1. Superimposition of the Ru_4 core of **8''**

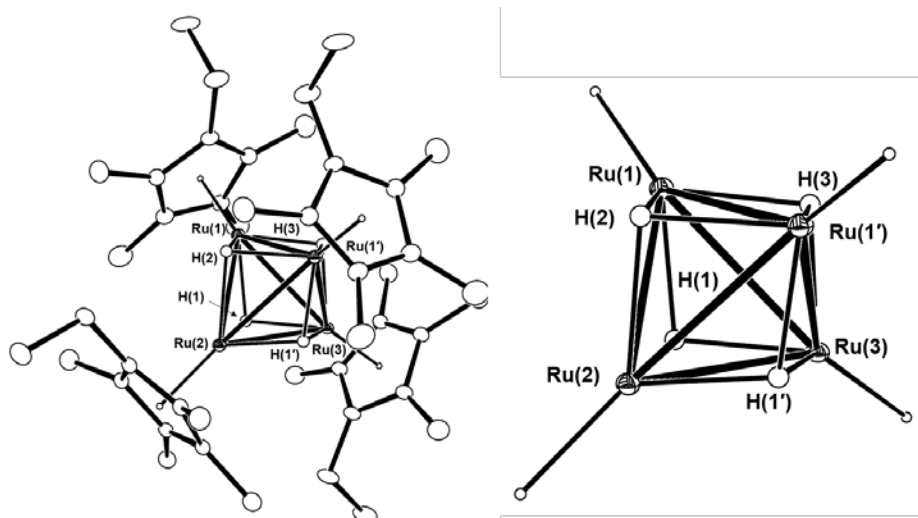


Figure S-7. ORTEP diagram of $[(\text{Cp}^{\text{Et}}\text{Ru})_4\text{H}_4]$ (**10'**), with thermal ellipsoids drawn at 30% probability (left), and the expanded view of the Ru_4 core of **10'** (right).. Hydrogen atoms on the Cp^{Et} groups were omitted for clarity.

Table S-6. Selected bond lengths (Å) and angles (deg) of **10'**

Ru(1)–Ru(1')	2.7868(3)	Ru(1)–Ru(2)	2.7883(3)	Ru(1)–Ru(3)	2.7922(2)
Ru(2)–Ru(3)	2.7941(3)				
Ru(1')–Ru(1)–Ru(2)	60.063(4)	Ru(1')–Ru(1)–Ru(3)	60.017(4)	Ru(2)–Ru(1)–Ru(3)	60.091(7)
Ru(1)–Ru(2)–Ru(1')	59.873(8)	Ru(1)–Ru(2)–Ru(3)	59.886(6)	Ru(1)–Ru(3)–Ru(1')	59.964(9)
Ru(1)–Ru(3)–Ru(2)	60.023(7)				

2. ^1H and ^{13}C NMR spectra of **5-BF₄**, **5-BPh₄**, **7-BF₄**, **7-BPh₄**, **8**, **8'**, **10**, and **10'**

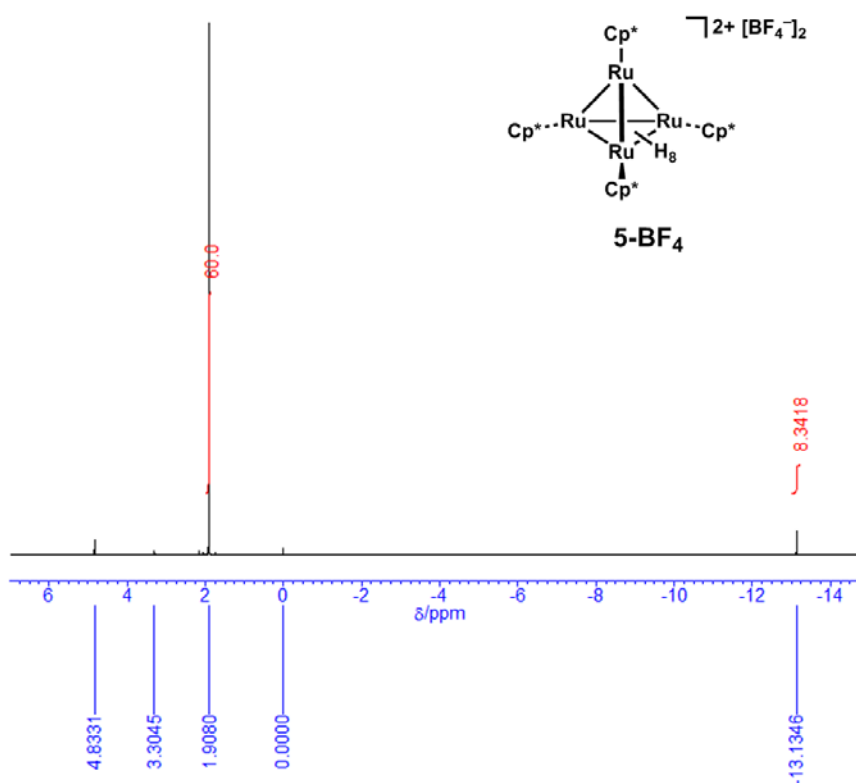


Figure S-8. ^1H NMR spectrum of $[(\text{Cp}^*\text{Ru})_4\text{H}_8]^{2+}(\text{BF}_4^-)_2$ (**5-BF₄**) (methanol-*d*₄, 400 MHz, 25 °C)

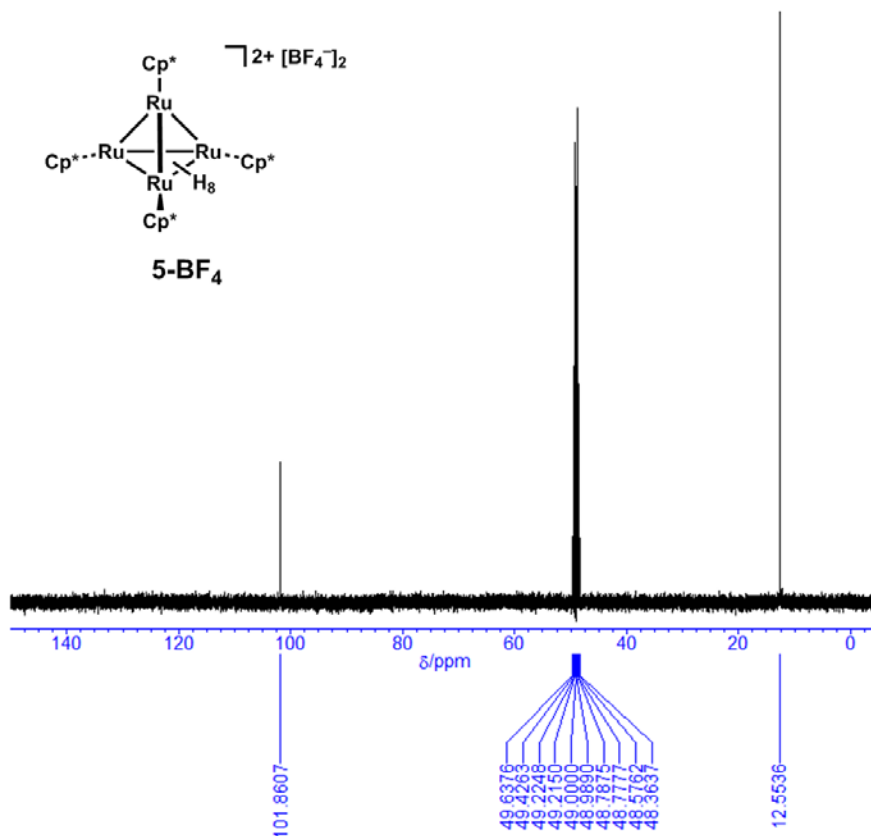


Figure S-9. $^{13}\text{C}\{^1\text{H}\}$ NMR spectrum of $[(\text{Cp}^*\text{Ru})_4\text{H}_8]^{2+}(\text{BF}_4^-)_2$ (**5-BF₄**) (methanol-*d*₄, 400 MHz, 25 °C)

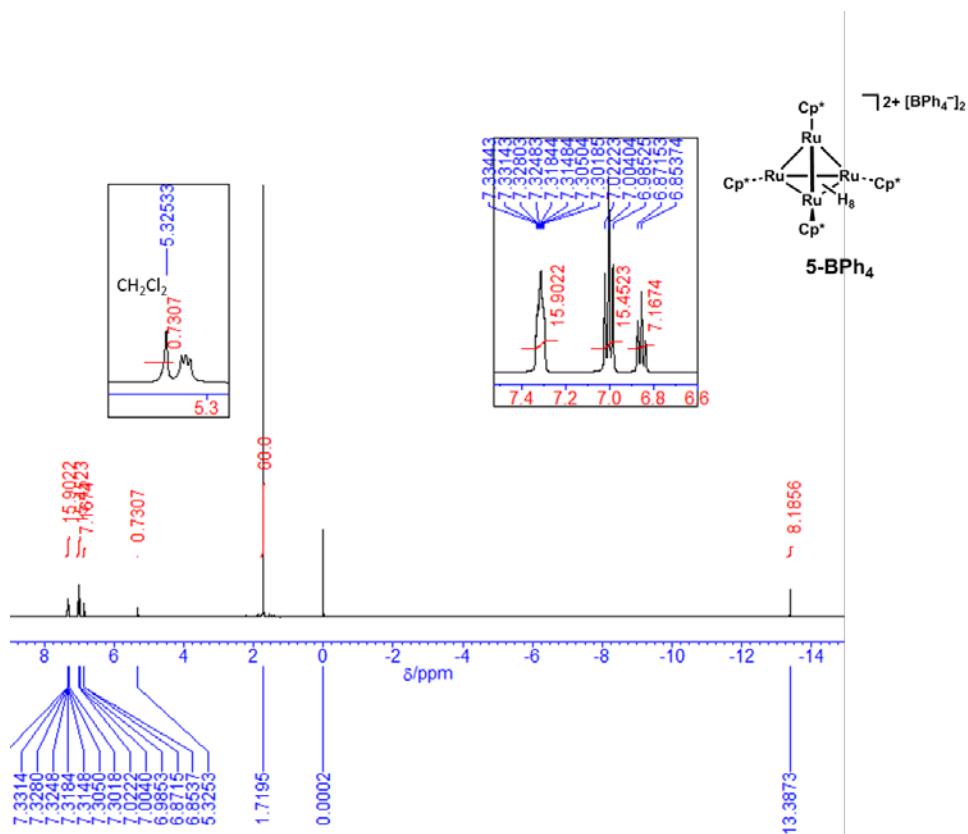


Figure S-10. ^1H NMR spectrum of $[(\text{Cp}^*\text{Ru})_4\text{H}_8]^{2+}(\text{BPh}_4^-)_2$ (**5-BPh₄**) (CD_2Cl_2 , 400 MHz, 25 °C)

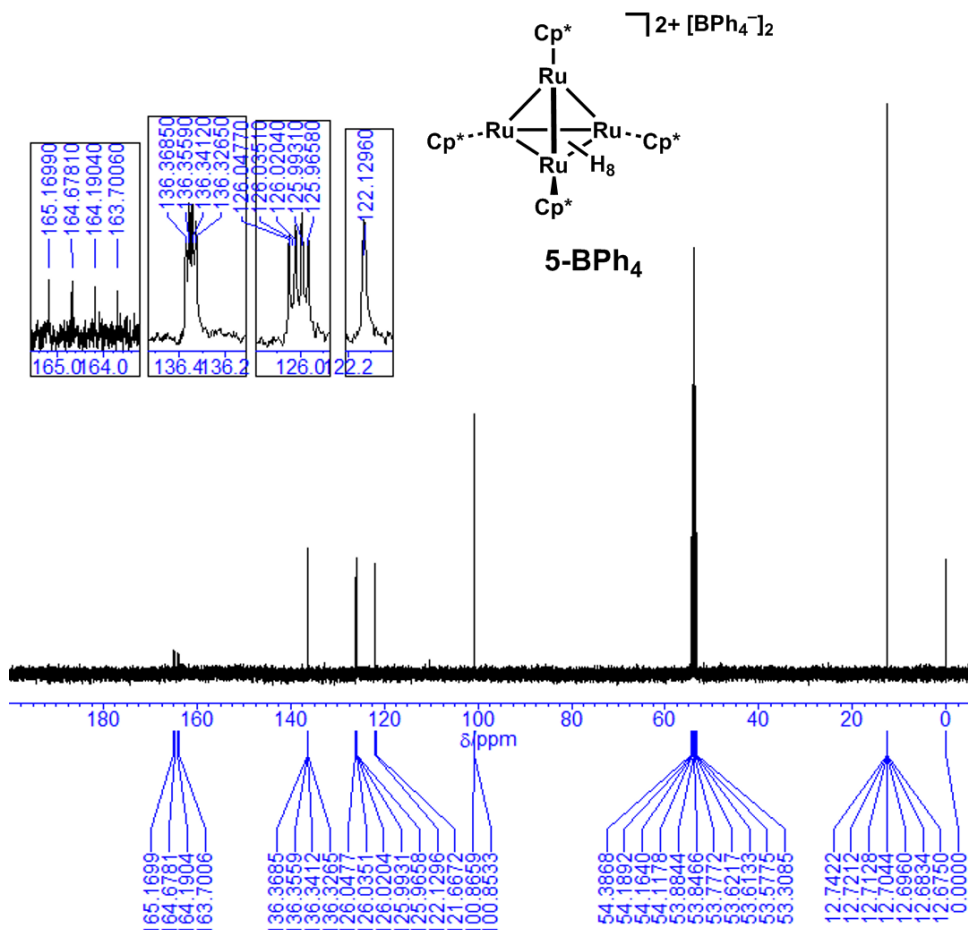


Figure S-11. $^{13}\text{C}\{^1\text{H}\}$ NMR spectrum of $[(\text{Cp}^*\text{Ru})_4\text{H}_8]^{2+}(\text{BPh}_4^-)_2$ (**5-BPh₄**) (CD_2Cl_2 , 400 MHz, 25 °C)

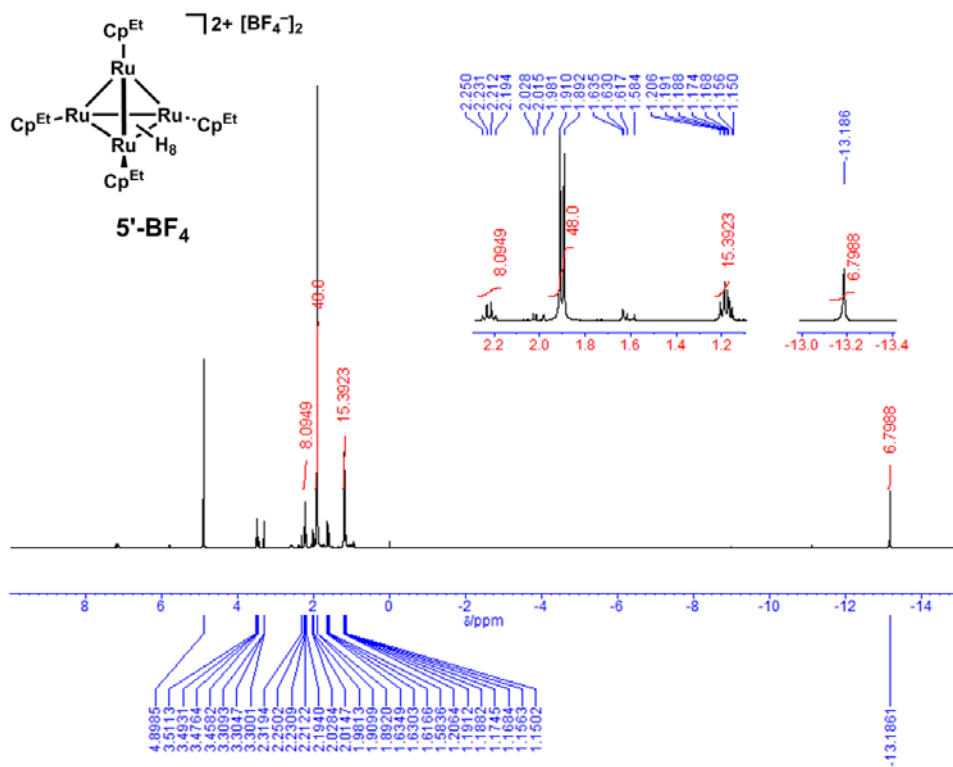


Figure S-12. ¹H NMR spectrum of $[(Cp^{Et}Ru)_4H_8]^{2+}(BF_4^-)_2$ (**5'-BF₄**) (methanol-*d*₄, 400 MHz, 25 °C)

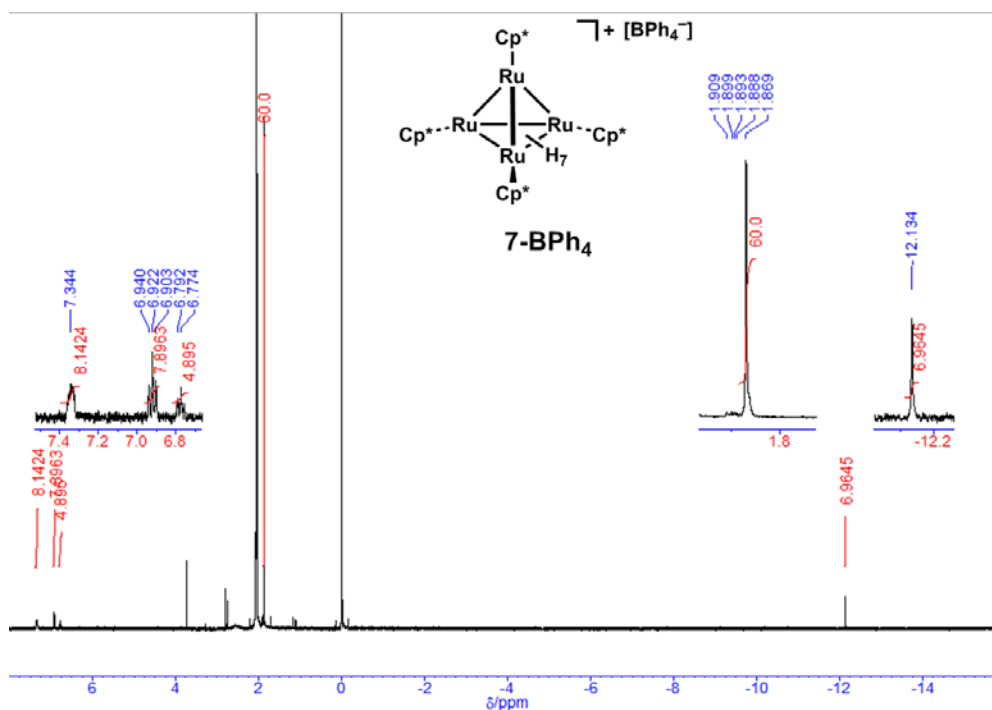


Figure S-15. ^1H NMR spectrum of $[(\text{Cp}^*\text{Ru})_4\text{H}_7]^+(\text{BPh}_4^-)$ (**7-BPh₄**) (methanol-*d*₄, 400 MHz, 25 °C)

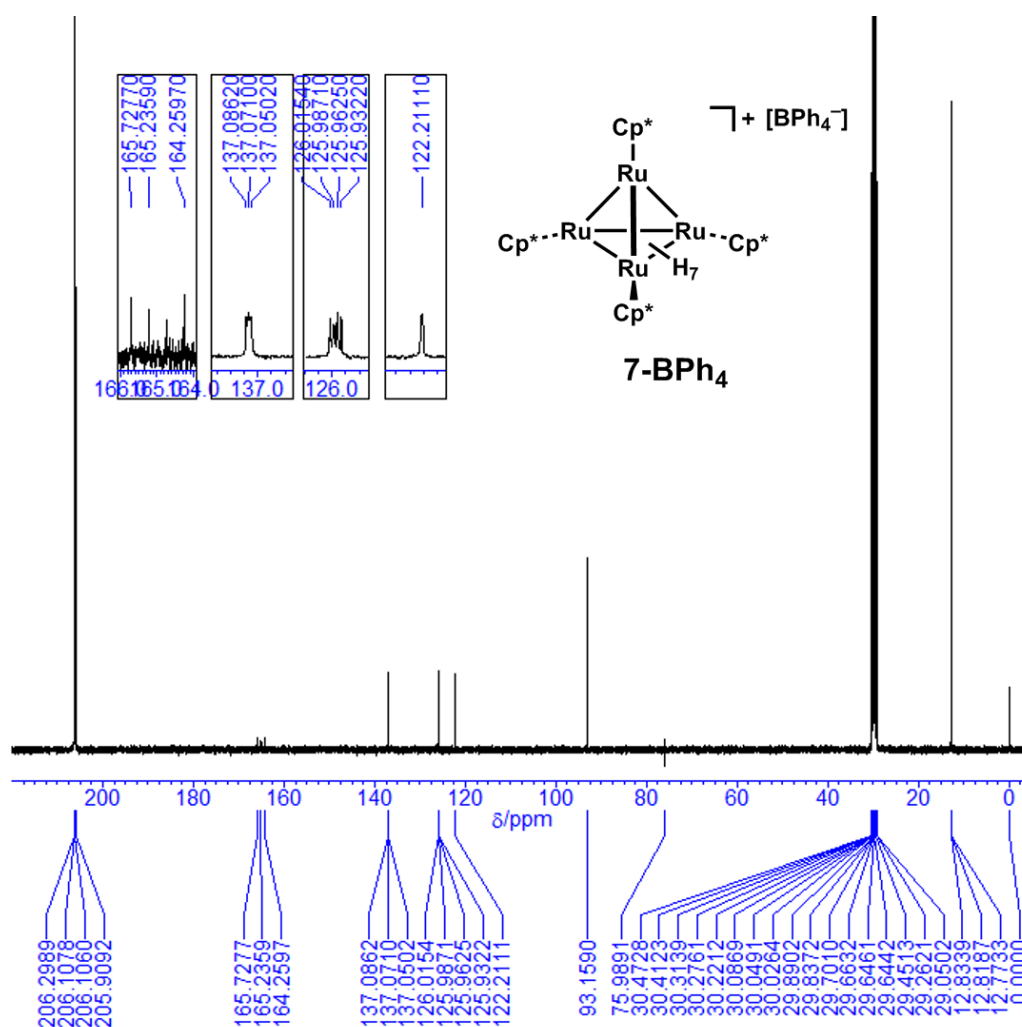


Figure S-16. $^{13}\text{C}\{^1\text{H}\}$ NMR spectrum of $[(\text{Cp}^*\text{Ru})_4\text{H}_7]^+(\text{BPh}_4^-)$ (**7-BPh₄**) (acetone-*d*₆, 100 MHz, 25 °C)

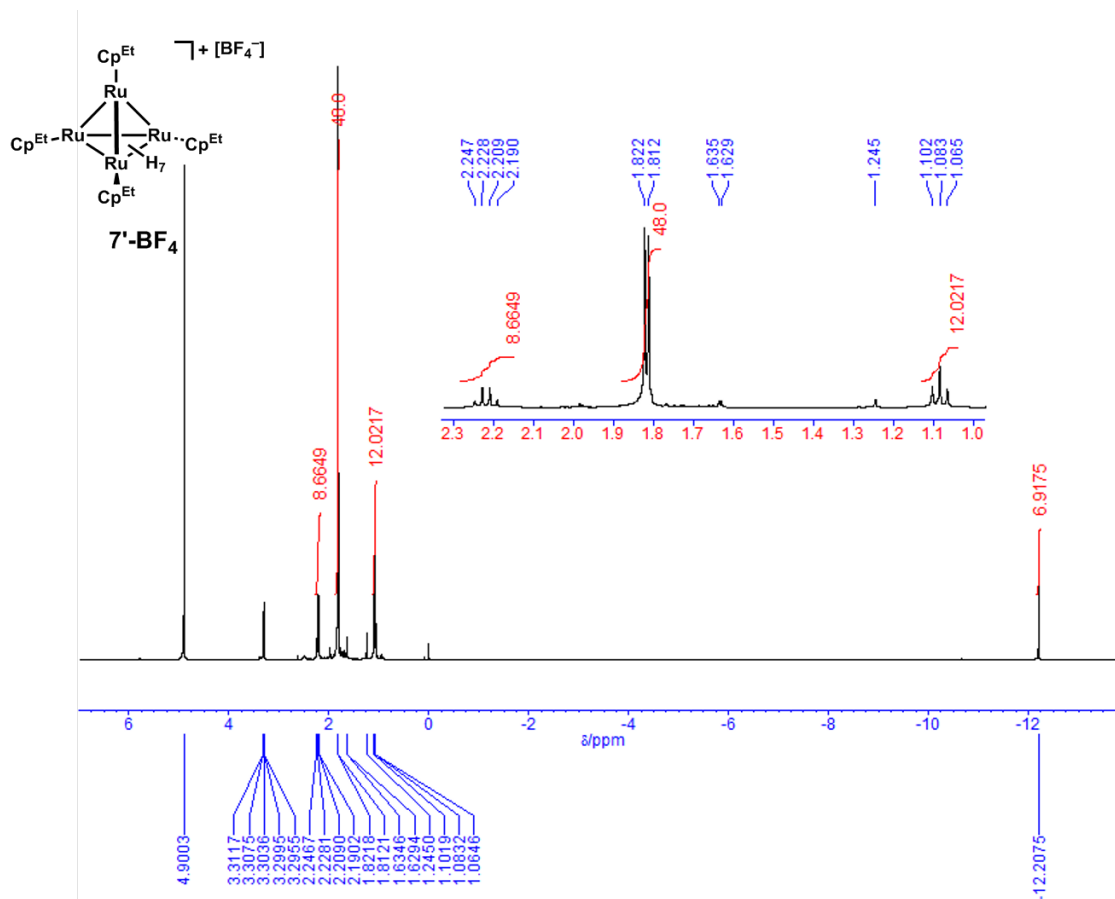


Figure S-17. ¹H NMR spectrum of [(Cp^{Et}Ru)₄H₇]⁺(BF₄⁻) (**7'-BF₄**) (methanol-*d*₄, 400 MHz, 25 °C)

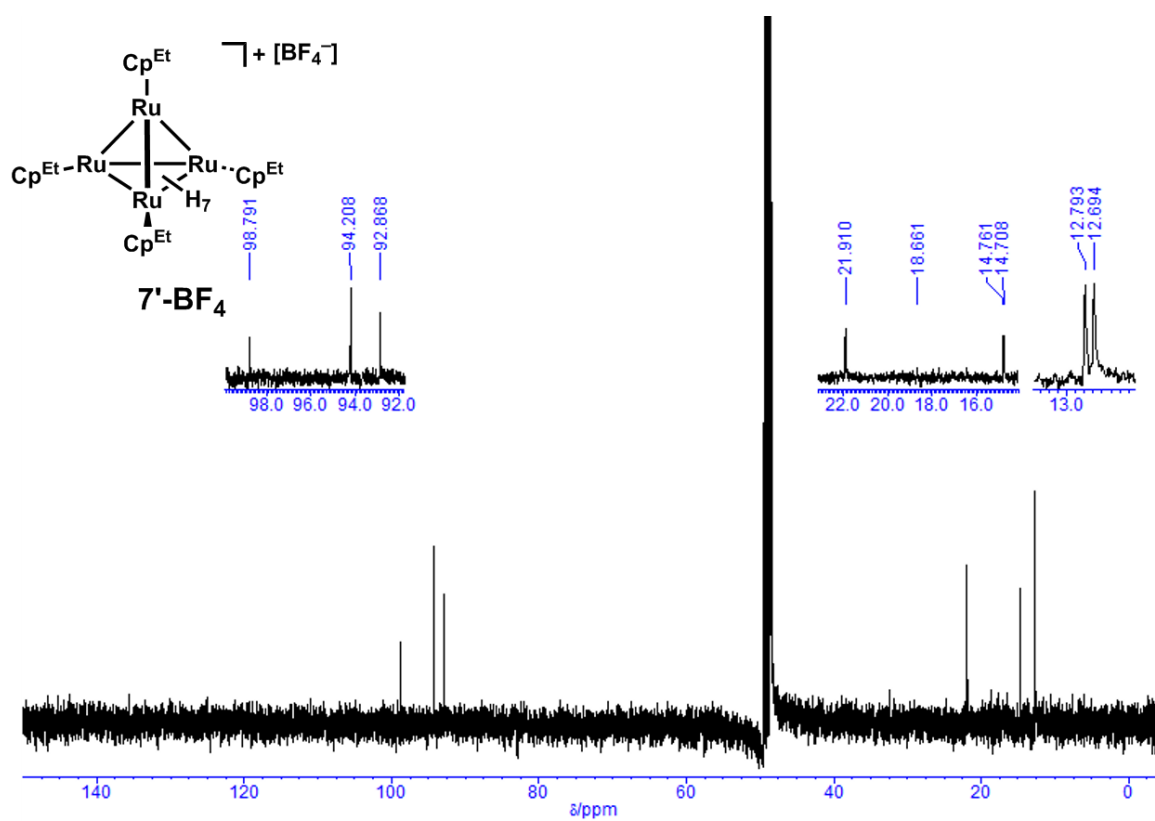
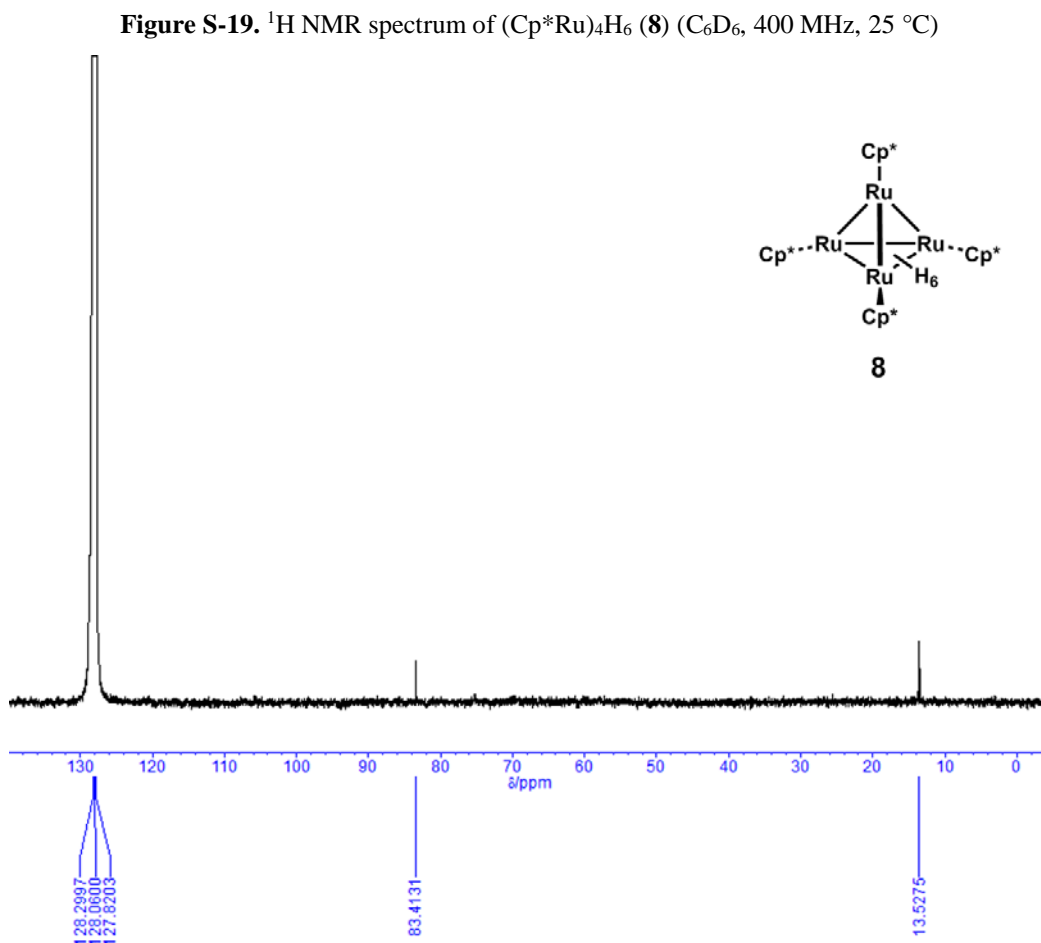
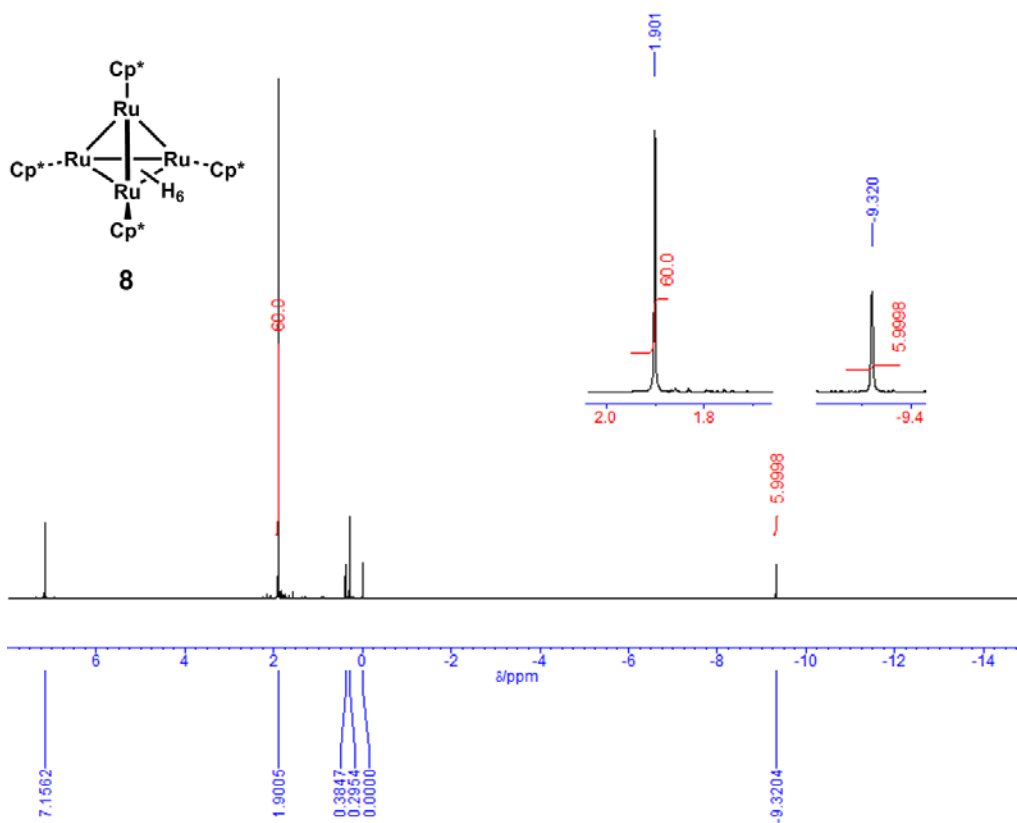


Figure S-18. ¹³C{¹H} NMR spectrum of [(Cp^{Et}Ru)₄H₇]⁺(BF₄⁻) (**7'-BF₄**) (methanol-*d*₄, 100 MHz, 25 °C)



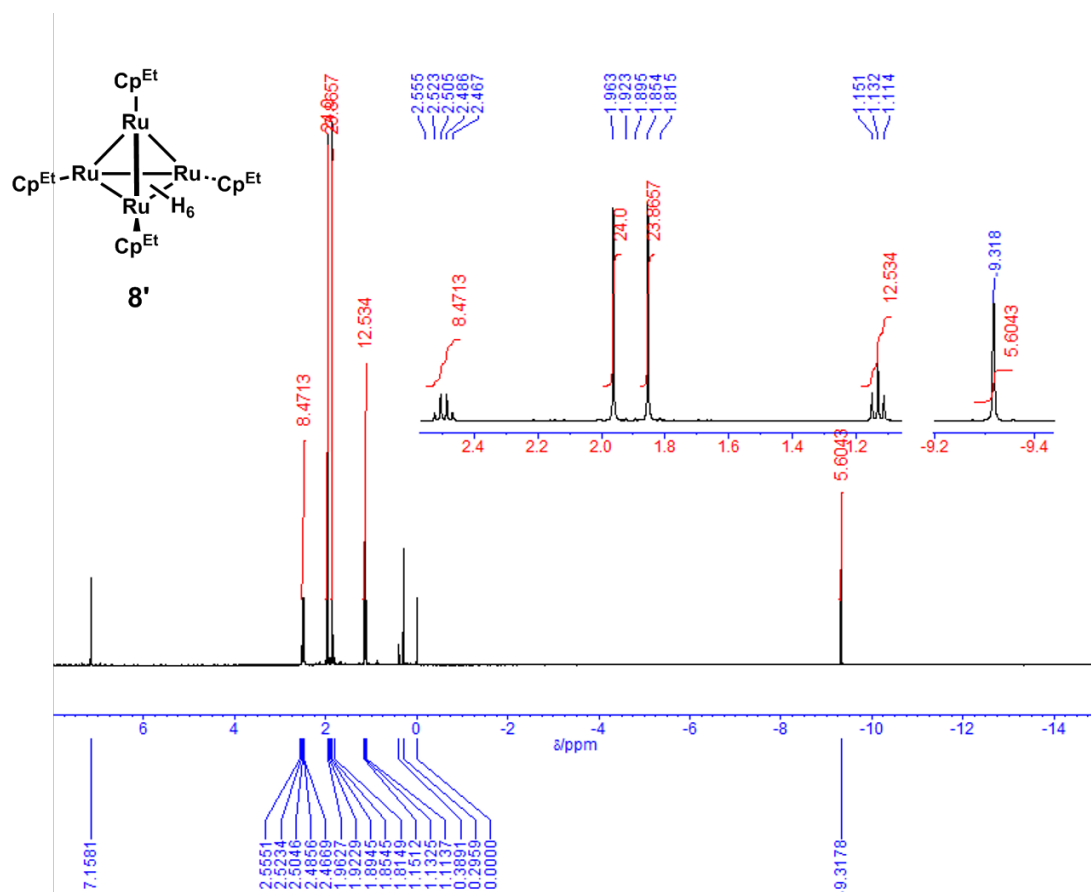


Figure S-21. ^1H NMR spectrum of $(\text{Cp}^{\text{Et}}\text{Ru})_4\text{H}_6$ ($8'$) (C_6D_6 , 400 MHz, 25 °C)

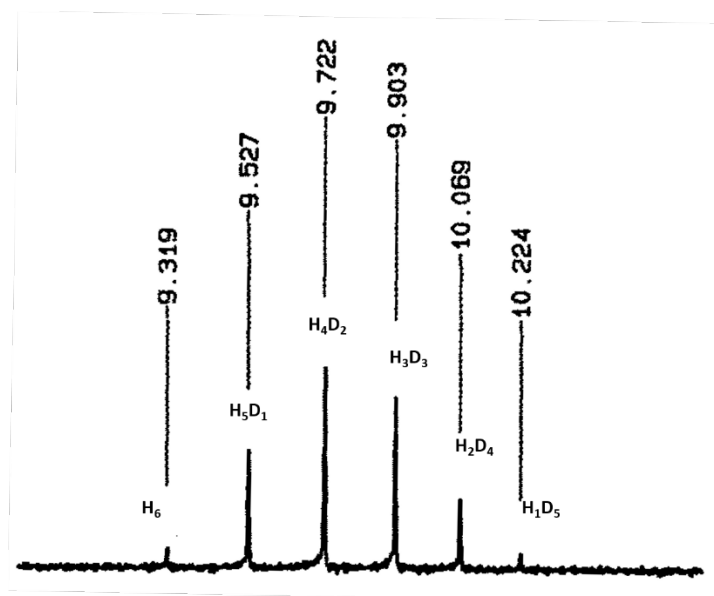


Figure S-22. Hydride signals of isotopomers of $8'$, $(\text{Cp}^{\text{Et}}\text{Ru})_4\text{H}_n\text{D}_{6-n}$ ($n = 1 - 6$), obtained upon heating at 100 °C in C_6D_6 for 60 h.

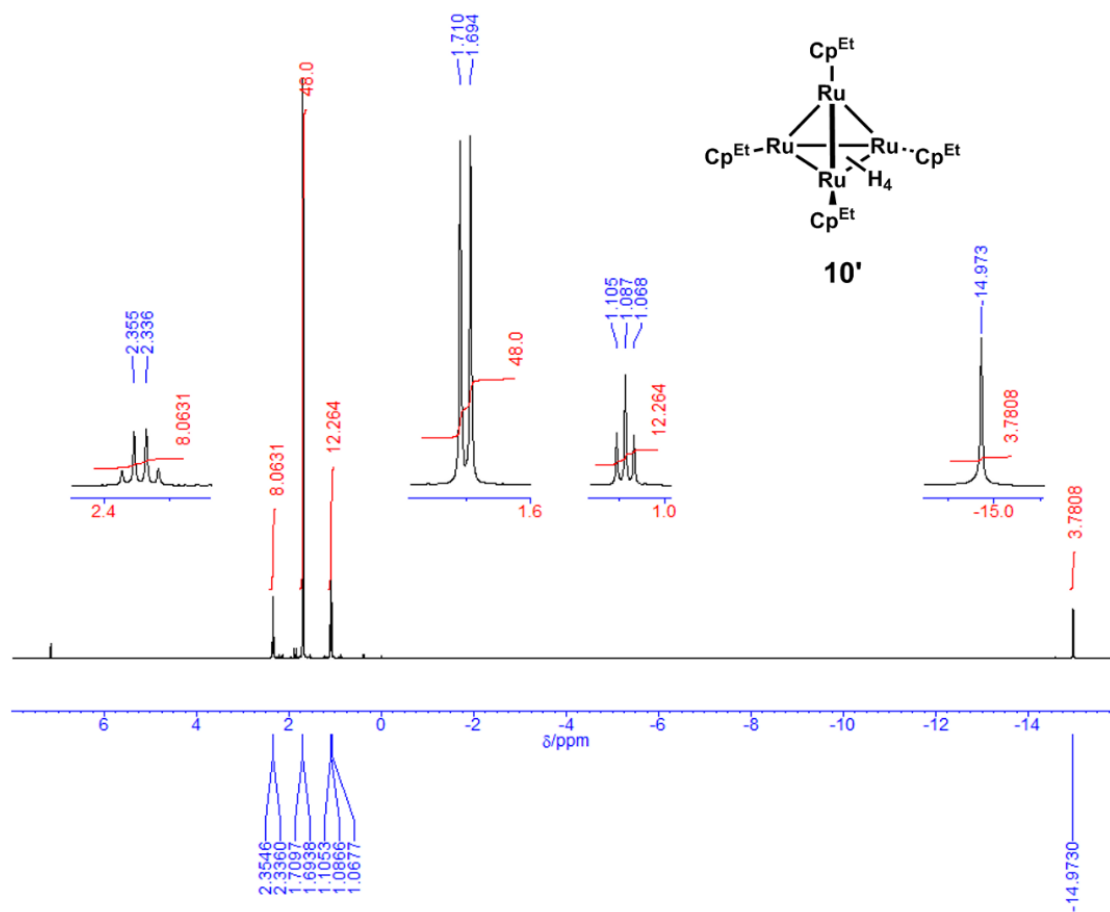


Figure S-23. ^1H NMR spectrum of $(\text{Cp}^{\text{Et}}\text{Ru})_4\text{H}_4$ (**10'**) (C_6D_6 , 400 MHz, 25 °C)

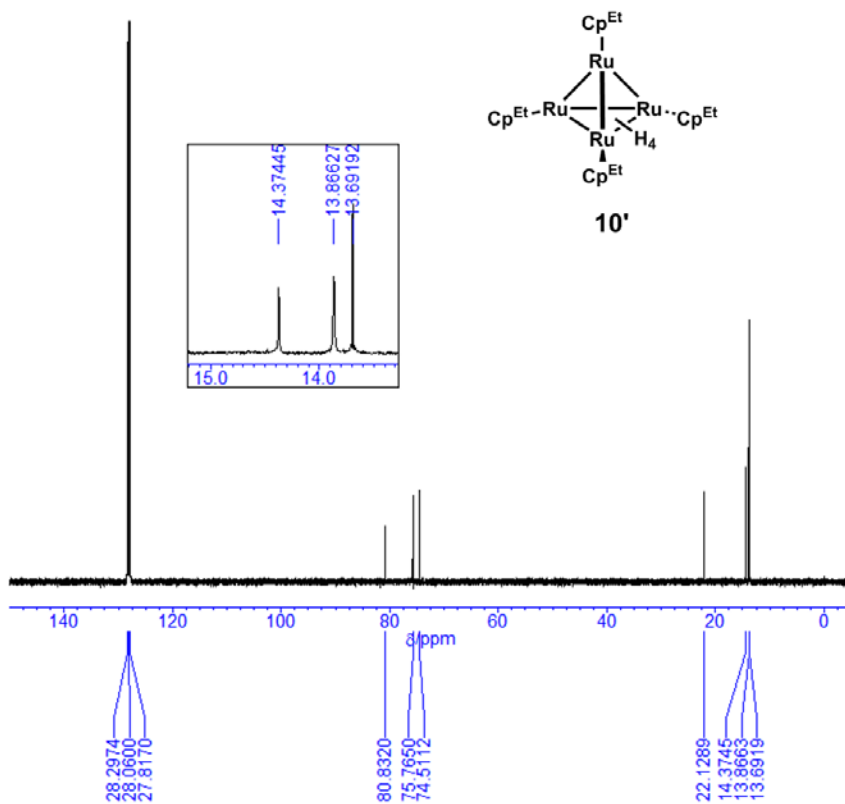


Figure S-24. $^{13}\text{C}\{^1\text{H}\}$ NMR spectrum of $(\text{Cp}^{\text{Et}}\text{Ru})_4\text{H}_4$ (**10'**) (C_6D_6 , 100 MHz, 25 °C)

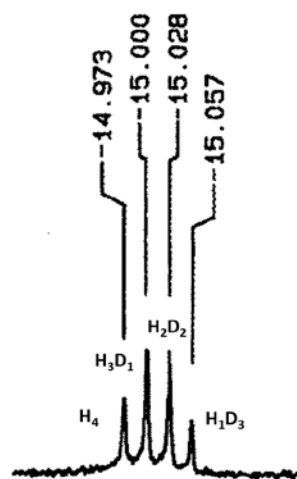


Figure S-25. Hydrido signals of isotomers of **10'**, $(\text{Cp}^{\text{Et}}\text{Ru})_4\text{H}_n\text{D}_{4-n}$ ($n = 1 - 4$), obtained upon heating at 140 °C in C_6D_6 for 24 h

3. Results of DFT calculations for 5''-A, 5''-B, 7'', 8'', and 10''

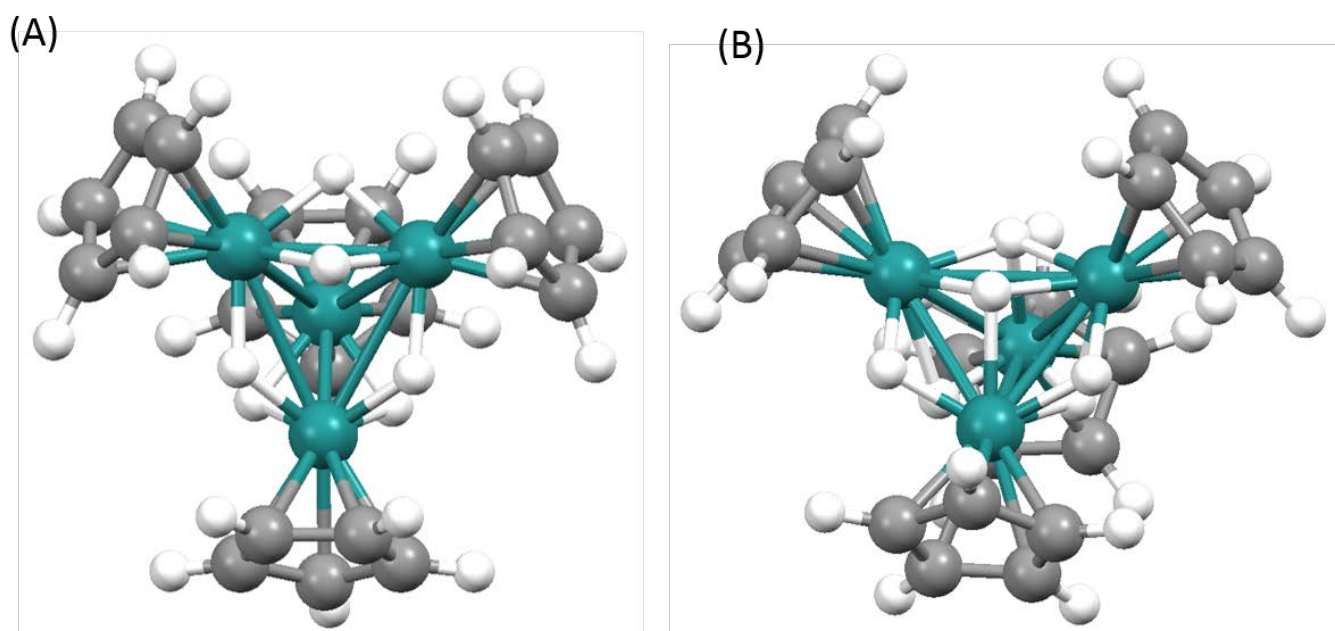


Figure S-26. Optimized structure of $[(\text{CpRu})_4\text{H}_8]^{2+}$ (A) 5''-A, (B) 5''-B

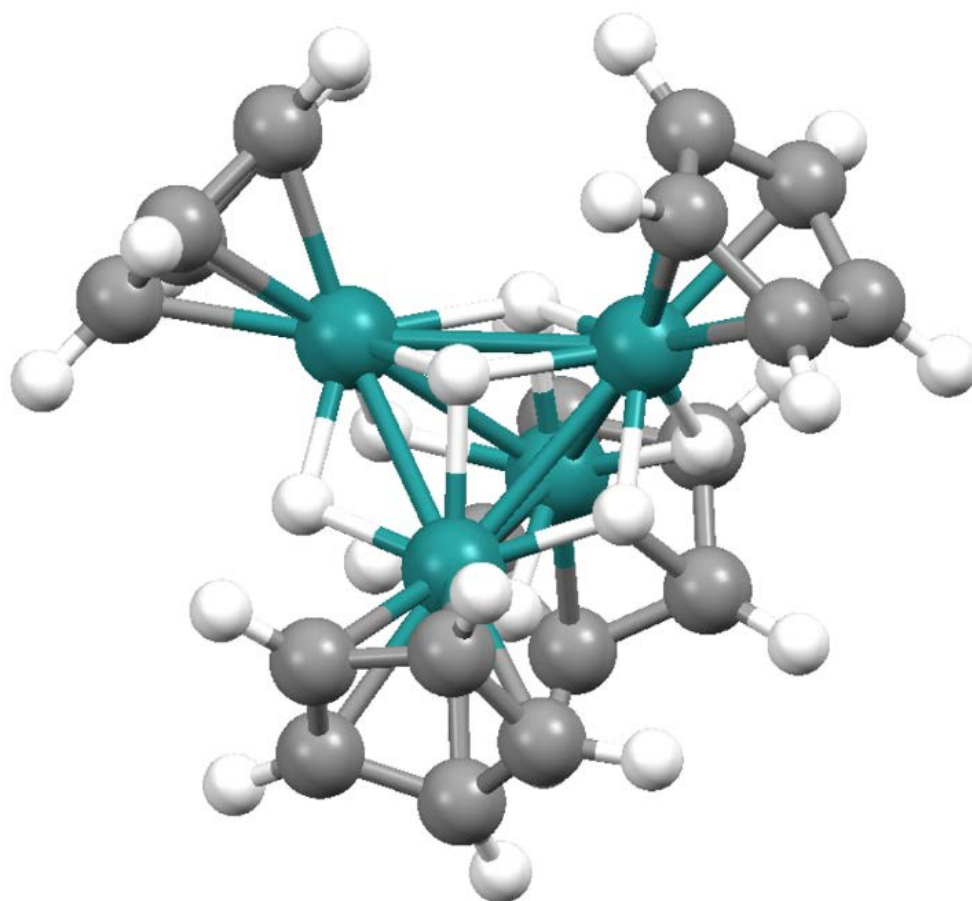


Figure S-27. Optimized structure of $[(\text{CpRu})_4\text{H}_7]^+$ (7'')

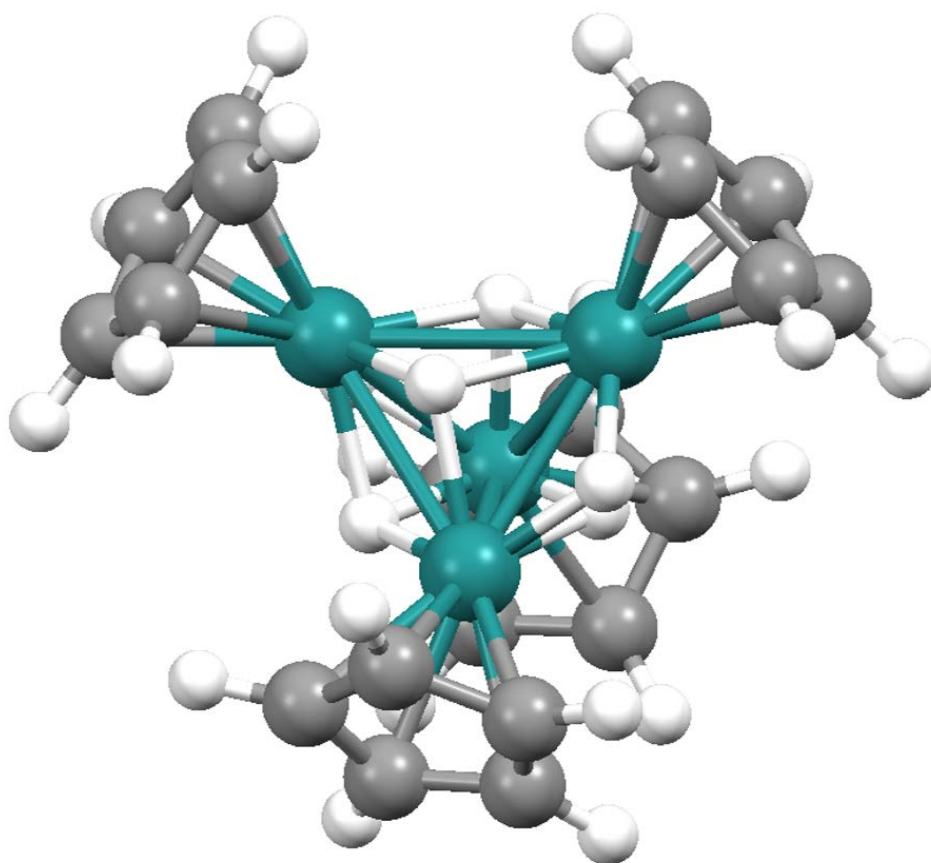


Figure S-28. Optimized structure of [(CpRu)₄H₆] (**8''**)

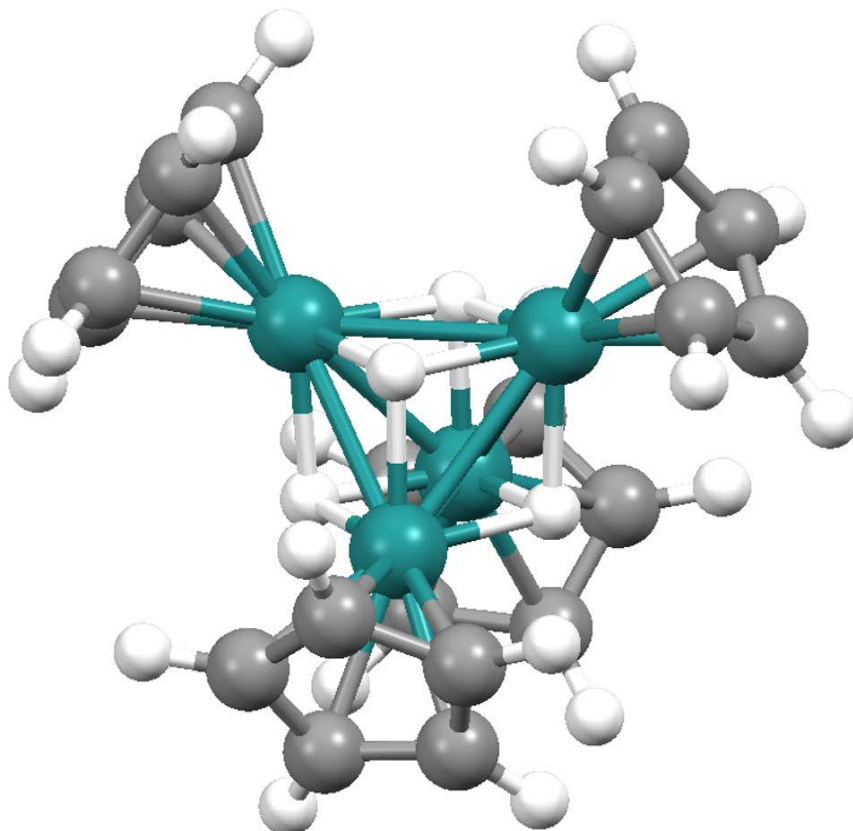


Figure S-29. Optimized structure of [(CpRu)₄H₄] (**10''**)

